Journal of Membrane Science 423–424 (2012) 209–214

Contents lists available at SciVerse ScienceDirect

Journal of Membrane Science

journal homepage: www.elsevier.com/locate/memsci

Copolymerization of methyl methacrylate and vinylbenzyl chloride towards alkaline anion exchange membrane for fuel cell applications

Yanting Luo [a], Juchen Guo [b,*], Yihang Liu [a], Qian Shao [c], Chunsheng Wang [a], Deryn Chu [d]

[a] Department of Chemical & Biomolecular Engineering, University of Maryland, College Park, MD 20742, USA
[b] Department of Chemical and Environmental Engineering, University of California Riverside, Riverside, CA 92521-0144, USA
[c] Department of Chemistry, University of Maryland, College Park, MD 20742, USA
[d] Sensors and Electron Device Directorate, US Army Research Laboratory, Adelphi, MD 20783, USA

ARTICLE INFO

Article history:
Received 18 May 2012
Received in revised form
7 August 2012
Accepted 9 August 2012
Available online 22 August 2012

Keywords:
Alkaline fuel cells
Alkaline anion exchange membranes
Emulsion polymerization
Crosslinking

ABSTRACT

Our previous studies demonstrated great potential of methyl methacrylate and vinylbenzyl chloride based copolymer electrolytes for alkaline fuel cell applications. In this study, a number of factors including polymer composition drift, molecular weight, and polymer crosslinking is investigated to understand their effects and to precisely control the electrolyte properties including conductivity, mechanical strength, and water mass-uptake. This investigation demonstrated a controllable polymerization procedure of poly (methyl methacrylate-co-vinylbenzyl chloride) membrane with tunable and balanced properties, which is promising for the alkaline fuel cell technology.

1. Introduction

Alkaline fuel cell (AFC) is one of the oldest fuel cell technologies developed extensively in 1950s for the space programs [1]. However, the severe CO_2 contamination and hazardous corrosion from concentrated liquid KOH electrolyte has limited conventional AFC applications, although AFCs have advantages over proton exchange membrane fuel cells in reducing cost by using non-noble metal electrode catalysts [2] and in fast reaction kinetics for both fuel oxidation and oxygen reduction reactions in alkaline medium [3].

The AFC technology has been revived due to recent advancement in alkaline anion exchange membrane (AAEM). The use of AAEM eliminates potassium carbonate precipitation on the electrodes, reduces KOH corrosion, and ensures the compact structure for portable electronic device and vehicles. Therefore, AAEM was extensively investigated for the last decade. To date, the current AAEM synthesis can be categorized into two types: functionalization of existing polymers and bottom-up synthesis of functional monomers. For the former, the precursor polymers include polysulfone [4], poly (arylene ether sulfone) [5], polyetherketone [6], poly (ether imide) [7], polyethersulfone cardo [8], poly(phthalazinon ether sulfone ketone) [9], poly(dimethyl phenylene oxide) [10], and poly(phenylene) [11]. The functionalization typically includes consecutive chloromethylation and quaternization, followed by anion exchange and membrane processing. The functionalized membranes can also be crosslinked to reduce water uptake and to improve mechanical strength of the membranes. The investigated crosslinking systems include photo-crosslinked poly (vinyl methylimidazolium iodide-co-styrene-co-acrylonitrile-co-divinylbenzene) [12]; chloroacetylated poly(2,6-dimethyl-1,4-phenylene oxide) (PPO) and bromomethylated PPO via Friedel-Crafts reaction [13]; glutaraldehyde [14], glyoxal [15] and diethylene glycol diglycidyl ether [16] crosslinked chitosan AAEMs; thtraphenylolethane glycidyl ether crosslinked poly (arylene ether sulfone) [17]; and allyl glycidyl ether crosslinked poly (epichlorhydrin) [18]. The second category of AAEMs is copolymers synthesized from specific functional monomers. In those copolymers, a part of the polymer chain serves as the hydrophobic portion to give mechanical strength of the membrane while the rest portion is hydroxide ion conducting after functionalization. Those novel copolymers include poly (methyl methacrylate-co-ethyl acrylate-co-vinylbenzyl chloride) [19], tetraalkylammonium functionalized polyethylene, [20] and our previously developed quaternized poly (methyl methacrylate-co-butyl acrylate-co-vinylbenzyl chloride) (QPMBV) [21–23].

The QPMBV AAEM fuel cells in our previous study demonstrated maximum power density of 180 mW cm^{-2} [22] and 420 h continuous operation under 75 mA cm^{-2} discharge current after crosslinking [24]. The focus of this study is to investigate a

* Corresponding author. Tel.: +1 951 827 6472.
E-mail address: jguo@engr.ucr.edu (J. Guo).

0376-7388/$ - see front matter © 2012 Elsevier B.V. All rights reserved.
http://dx.doi.org/10.1016/j.memsci.2012.08.016

number of fundamental polymerization factors in detail, and to understand their effects on the AAEM properties. Specifically, we focus on (1) the role of monomer composition drift adjustment in electrochemical conductivity, (2) the effect of molecular weight enhancement on mechanical strength, and (3) crosslinking mechanism of divinylbenzene (DVB) crosslinker in AAEMs using atomic force microscopy (AFM).

2. Experimental

2.1. Miniemulsion copolymerization

Miniemulsion polymerization was prepared by dispersing 30 g methyl methacrylate (MMA) and vinylbenzyl chloride (VBC) mixture and 0.12 g hexadecane (HD) into 150 ml aqueous sodium dodecyl sulfate (SDS) solution by ultra-sonication. The polymerization was initiated by injection of potassium persulfate (KPS) into the miniemulsion at 70 °C under nitrogen protection. The reaction was terminated after 4 h by quenching in ice bath. The copolymer was filtered and dried in vacuum overnight. Monomer conversion was measured during the polymerization. Prior to the polymerization, aluminum weight pans pre-loaded with trace amount of hydroquinone (as polymerization terminator) were weighted and recorded. During the polymerization, small amount of miniemulsion reaction content was drawn from the reactor flask from various intervals, and put in the aluminum pan and weighted. After completely drying the drawn miniemulsion content in vacuum oven overnight, the obtained residue (with the pan) was weighted again. The monomer conversion was calculated by gravimetric method using following equation

$$\text{conversion} = \frac{W_{dry} - W_{wet} \times (\text{SDS} + \text{KPS} + \text{HD})\text{wt}\%}{W_{wet} \times \eta} \quad (1)$$

where W_{dry} was the weight of the residue in the weighting plate; (SDS+KPS+HD) wt% is the total weight percentage of SDS, KPS, and HD in the reactant mixture; W_{wet} was the weight of the miniemulsion content drawn to the weight pan; and η is the weight percentage of monomers in the entire reactant mixture.

Copolymer composition of poly (methyl methacrylate-co-vinylbenzyl chloride) (PMV) was calculated based on ^{1}H-NMR (proton nuclear magnetic resonance, Bruker DRX-400 high resolution). GPC (gel permeation chromatography, Waters 2410 Refractive Index Detector) was employed to measure the molecular weight of PMV. DLS (dynamic light scattering) was used to determine the droplet size in the miniemulsion system.

2.2. Membrane processing

PMV was dissolved in dimethylformamide (DMF) to form a 5 wt% solution. Trimethylamine gas was bubbled through the solution for 2 h at 60 °C while stirring. The quaternized PMV (QPMV) was directly cast into a film on an aluminum plate, and dried inside of a sealed chamber in nitrogen environment at 60 °C overnight. For crosslinking, obtained QPMV solution in DMF was put into a flask with reflux condenser under nitrogen protection. A certain amount of DVB (0–10 wt% of the QPMV) was injected into the system. The crosslinking reaction was started by injecting azobisisobutyronitrile (AIBN, 1.5 mmol L^{-1} of the DMF solution) in the solution at 60 °C. The reaction was carried out at 60 °C for 24 h when the solution became visually more viscous. After crosslinking, the obtained solution was cast into a film. The obtained membranes were further dried in vacuum oven at 60 °C for 24 h, followed by soaking in 6 M KOH solution for overnight to exchange Cl^- to OH^-. The OH^- exchanged membrane was washed with DI water until pH of 7 was reached.

2.3. Morphology characterization

AFM (AppNano ACT-SS-10) was used to characterize the morphologies of the pure polymer membrane, quaternized membrane, and crosslinked quaternized membrane. Static mode of the cantilever with an n-type silicon tip was forced on the spin-coated membrane on silicon wafer to collect the image from a laser deflection.

2.4. Conductivity and mechanical properties tests

Anion conductivity of QPMV was measured using EIS (electrochemical impedance spectroscopy, Gamry Instruments 3000, Potentiostat/Galvanostat/ZRA) with the fixture of conductivity cell (BekkTech, BT-112). Four-probe method was employed for all the conductivity tests. The temperature and humidity in the conductivity cell were controlled using an Arbin fuel cell test station. Conductivity was calculated by

$$\sigma = \frac{l}{Rab} \quad (2)$$

where l is the membrane thickness, a is the membrane width, b is the membrane length and R is the resistance obtained from EIS.

The mechanical properties were measured using a dynamic mechanical analyzer (DMA, TA Instruments Q800) by tensile tests at room temperature. The stretch rate was 1 N min^{-1}. Water uptake was measured by gravimetric method, and calculated by

$$\text{uptake}\% = \frac{m_{wet} - m_{dry}}{m_{dry}} \times 100\% \quad (3)$$

where m_{wet} is the weight of the membrane after being saturated with water and m_{dry} is the weight of the dry membrane.

3. Results and discussion

3.1. Composition drift effect

Three PMV copolymers with various compositions were synthesized by miniemulsion copolymerization. Fig. 1 shows the

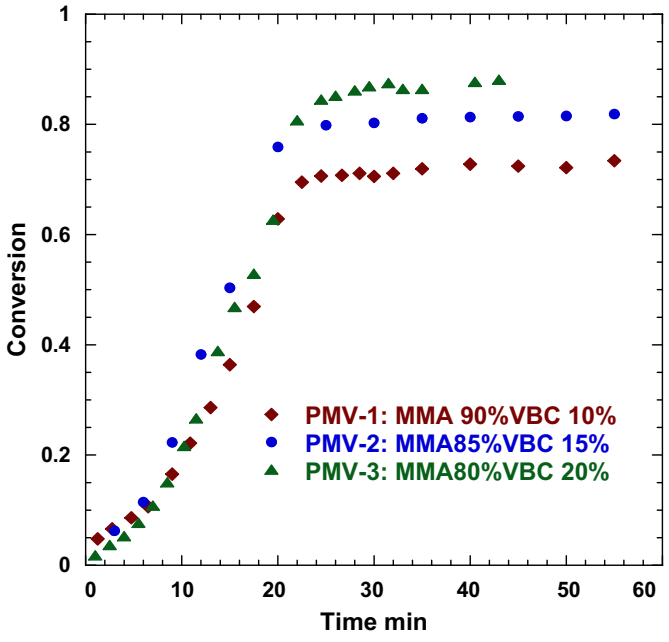

Fig. 1. Overall monomer conversion with various compositions in copolymerization.

overall conversion of monomer as function of reaction time. It was obvious that the conversion for all three samples increased rapidly in the initial polymerization time, and then leveled off after approximately 25 min. The difference in final conversion with various compositions could be attributed to the Trommsdroff effect [25], which was common in MMA included polymerization for its self-acceleration phenomenon. As shown in Fig. 1, decrease in MMA component resulted in higher overall conversion of monomers.

The correlation between reactivity ratio of monomers and monomer concentration fraction could be expressed as Eq. (4) [26], when the conversion of monomers was lower than 5% (in the first 5 min of reactions). In the low conversion range, the fraction of unreacted monomer in the system at an instant moment can be assumed to be the same as the initial monomer fraction. The monomer fraction in polymer can be simply obtained from integration of copolymer composition that measured from ^{1}H-NMR spectra.

$$r_2 = f_1^0\left[\frac{1}{F_1}\left(1+f_1^0 r_1\right)-1\right] \tag{4}$$

where r_2 is the reactivity ratio of VBC and r_1 is the reactivity ratio of MMA; f_1^0 is the initial monomer fraction of MMA in mixture of MMA and VBC; F_1 is the MMA composition in the copolymer calculated from ^{1}H-NMR spectra.

The Mayo–Lewis plot [26] is plotted in Fig. 2 based on Eq. (4) with 3 different initial monomer fractions (QPMV-1, 2, and 3 as in Table 1). The intersection point gives the value of reactivity ratios of MMA and VBC. The reactivity ratio indicates the relative preference of radical monomers reacting to its own kind over to the other monomer. It is shown in Fig. 2 that the reactivity ratios of both MMA and VBC are lower than 1 (approximately 0.3 and 0.7, respectively), indicating the tendency for a random copolymer. Moreover, r_1 was two times lowers than r_2, indicating that VBC was more likely to be polymerized in the initial stage of the copolymerization, while MMA was likely to be self-polymerized later in the system.

Once reactivity ratios were obtained, copolymer composition drift from the unreacted monomers fraction could be established by Eqs. (5) and (6). f_1 is the instant unreacted MMA monomer fraction in the system, which could be related to conversion through the mass balance between the monomers and the obtained copolymer, as rearranged in Eq. (5). F_1 is the MMA fraction in the copolymer as expressed in Eq. (6).

$$C = 1-\left(\frac{f_1}{f_1^0}\right)^{(r_2/(1-r_2))}\left(\frac{1-f_1}{f_2^0}\right)^{(r_1/1-r_1)} \times\left(\frac{f_1^0-((1-r_2)/(2-r_1-r_2))}{f_1-((1-r_2)/(2-r_1-r_2))}\right)^{(1-r_1r_2/(1-r_1)(1-r_2))} \tag{5}$$

where f_1^0 and f_2^0 are the initial monomer fraction of MMA and VBC respectively.

$$F_1 = \frac{f_1^0-(1-C)f_1}{C} \tag{6}$$

From Eqs. (5) and (6), f_1 and F_1 can be plotted as functions of C, as shown in Fig. 3. The calculated F_1 vs. C was consistent with the ^{1}H-NMR measurements from the conversion test samples. From Fig. 3, the important information was that the resulted copolymer composition after polymerization was determined when f_1 approaching to 1 and conversion reaching its limit. Moreover, the MMA composition in the copolymer was all around 5% less than the initial MMA fraction in the monomer mixture, as denoted in Fig. 3.

Therefore, the simple correlation between copolymer composition and the initial monomer fraction was disclosed in Fig. 3. At the very beginning of the polymerization, copolymer composition was around 15% lower than the initial monomer fraction, as the conversion was as small as to zero. As the polymerization approached to the end of conversion, the composition of the copolymer became all around 5% lower than the initial monomer fraction. This investigation established the simple relation between composition in copolymer and the monomer fraction, which guided us to design the composition in copolymer as needed by initial adjustment of monomer fraction, not only qualitatively but also quantitatively.

The properties of the obtained membranes including conductivity and water uptake at room temperature were listed in Table 1. The ionic conductivity of QPMV membranes as function of temperature is shown in Fig. 4. The conductivity in Fig. 4 demonstrated that increasing in VBC component enhanced the conductivity. The highest conductivity could reach 0.1 S cm^{-1} for the sample with 20% VBC at 80 °C. However, the water uptake results indicated that all three membranes have high swelling ratios increased with increasing VBC content, which made them unrealistic for fuel cell operation. To address this problem, we enhanced the molecular weight and crosslinked the polymer to improve the mechanical properties. Initial monomer mixture with 10 mol% VBC and 90 mol% MMA was chosen to carried out the study, as it had the lowest water-uptake before improvement.

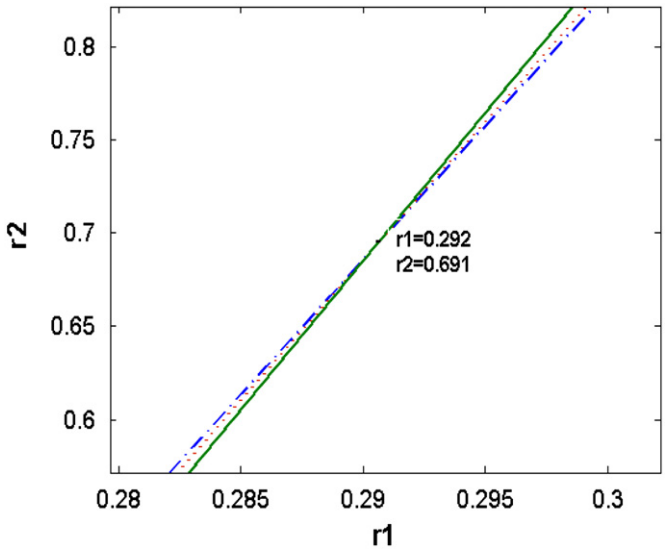

Fig. 2. Reactivity ratios for MMA and VBC (r_1: MMA; r_2: VBC).

3.2. Molecular weight optimization

Increasing molecular weight can effectively improve the mechanical strength of the QPMV membranes [21,22]. In this study, the effect of the concentration of initiator and surfactant used in copolymerization on the molecular weight was investigated.

As illustrated in Fig. 5, decreasing in KPS concentration, i.e. lower free radical concentration, certainly led to higher molecular weight. Less KPS initiators would have less primary free radicals available in the copolymerization system, while monomers concentration remained the same. Therefore, each polymer chain was enlarged by attaching more monomers, resulted in an increased molecular weight. It was shown in Fig. 5 that KPS concentration at 0.025 mol L^{-1} could result in a molecular weight of 4×10^6 g mol^{-1}. When KPS concentration was fixed at 0.025 mol L^{-1}, the concentration of surfactant, SDS, also demonstrated influence on molecular weight as shown in Fig. 6. Increase in SDS concentration would

Table 1
Properties of QPMVs.

Copolymer PMV and quaternized QPMV	Initial composition (MMA:VBC mol%)	Cross-linking (wt%)	Molecular weight (10^6 g/mol)	Conductivity water-saturated at RT 10^{-2} S/cm	Water-uptake (%)	Young's modulus (GPa)
1	90:10	–	2.5	1.72	197.0	2.3
2	85:15	–	2.4	1.80	362.3	2.2
3	80:20	–	2.4	1.89	646.3	2.4
4	90:10	–	4.1	1.69	186.1	2.7
5	90:10	–	6.6	1.73	190.8	3.3
6	90:10	5%	6.6	0.85	110.3	3.2
7	90:10	10%	6.6	0.80	63.1	3.3

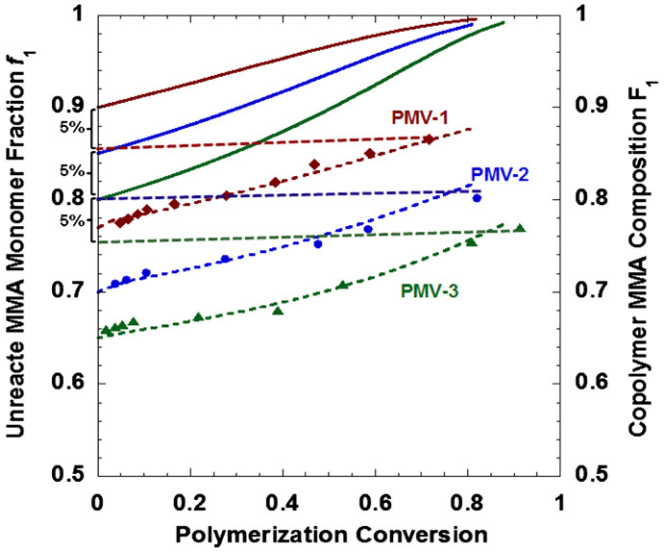

Fig. 3. Correlation of unreacted monomer fraction f_1 (solid line) and the composition in the resulted copolymer F_1 (dotted line) as a function of conversion C.

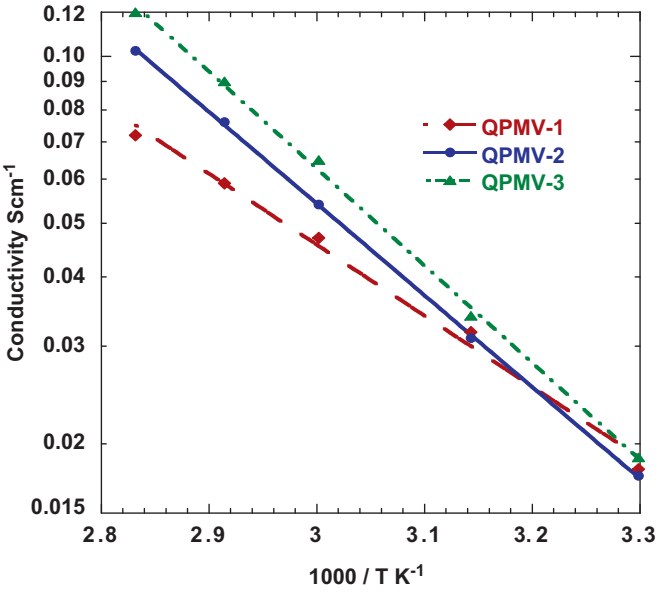

Fig. 4. Conductivities of PMVs with different compositions.

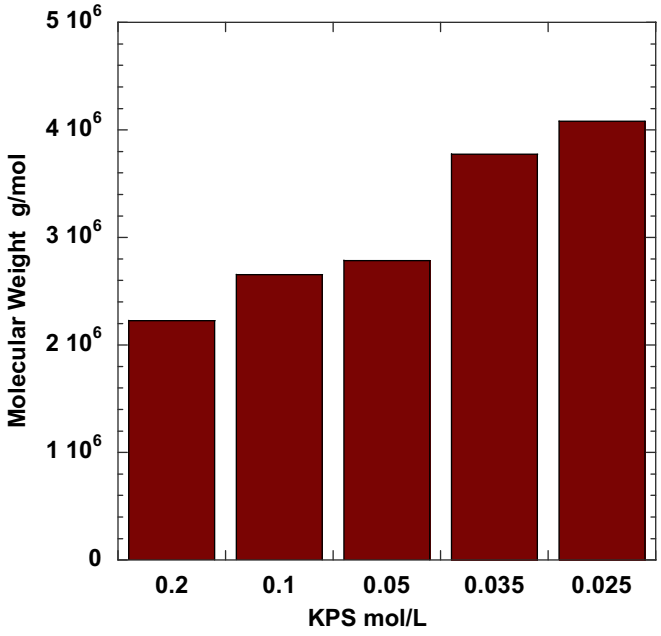

Fig. 5. Effect of KPS concentration on molecular weight.

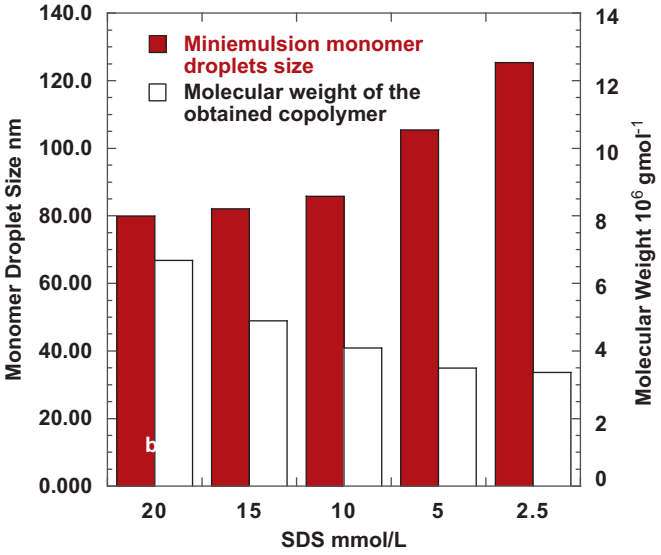

Fig. 6. Effects of SDS concentration at a fixed KPS concentration of 0.025 mol L^{-1}.

increase the molecular weight. More SDS in the system would decrease miniemulsion monomer droplet size, confirmed from DLS test as shown in Fig. 6. With droplet size decreased, the number of droplets increased. Therefore, the number of free radical relative to one droplet decreased, which was also resulted in less polymer chains with higher molecular weight.

After the optimization, the molecular weight could reach 6.6×10^6 g mol^{-1}. The morphology of this polymer was further characterized by AFM after spin coating as a thin film. Fig. 7a is the 3D topography of the optimized PMV and Fig. 7b is the 3D phase image, respectively. It was shown from Fig. 7 that the

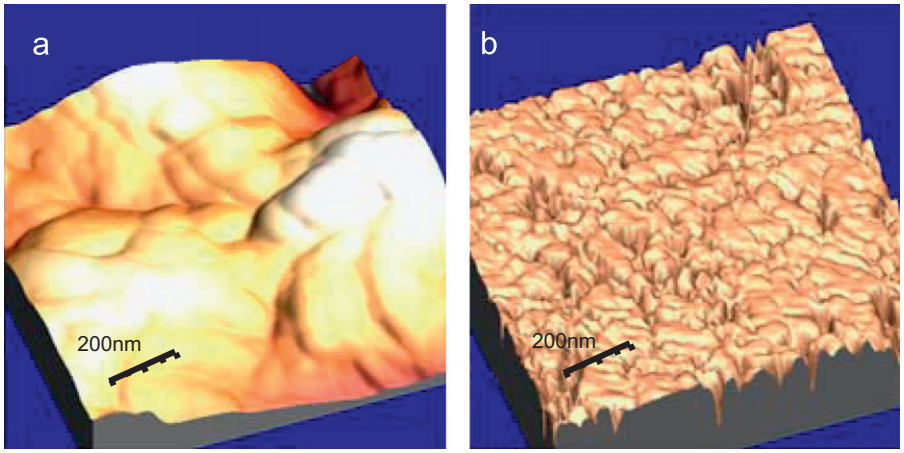

Fig. 7. AFM (a) 3D topography and (b) 3D phase images of optimized PMV.

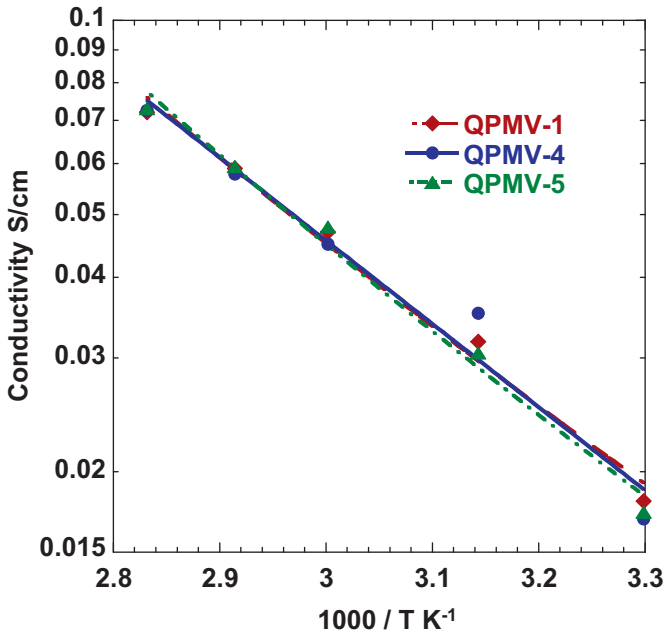

Fig. 8. Conductivities of QPMV membranes with different molecular weight.

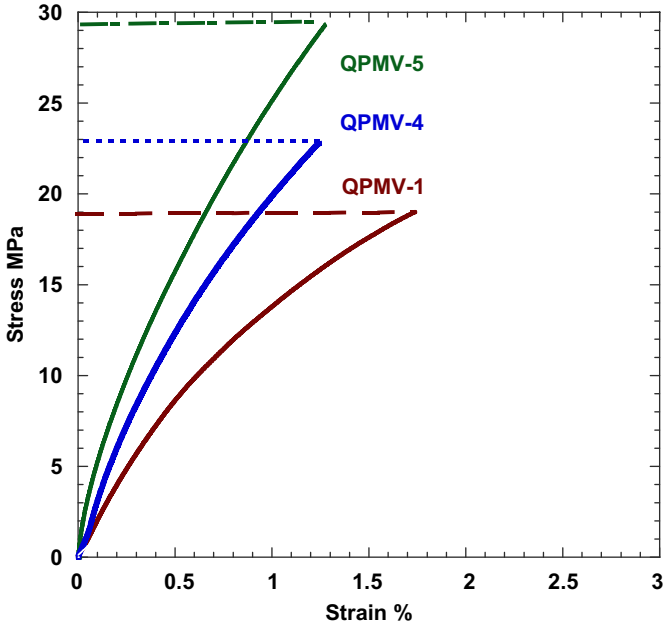

Fig. 9. Tensile tests for PMVs with different molecular weight.

copolymer could form homogeneously smooth and dense PMV membrane with little ionic channels, as compared to the membranes after processing and crosslinking, which would be discussed in detail in the next section.

The conductivity and mechanical strength of the QPMV membranes with same composition but different molecular weight were tested and shown in Figs. 8 and 9, respectively. The conductivities shown in Fig. 8 were measured at 80% relative humidity using a four-probe method under nitrogen protection. The conductivity results indicated that molecular weight of QPMV polymer did not change the ionic conductivities. However, both Young's modulus and tensile strength of the membranes were increased as the molecular weight increased as evidenced in Fig. 9. The optimized QPMV-5 had a highest Young's modulus of 3.3 GPa and the highest tensile strength of 29.5 MPa, which implied a strong and tough membrane material. The water uptakes were also listed in Table 1. It was shown that molecular weight did not influence much on water-uptake, which indicated that water-uptake was mostly dependent on the hydrophobic and hydrophilic composition. To further lower the water uptake, which was critical in fuel cell application, the crosslinking method was employed.

3.3. *Crosslinking QPMVs*

Crosslinking was proved to be an effective method to reduce water uptake and to enhance the mechanical properties of the AAEMs. In our previous study [24], PMV copolymer was crosslinked with DVB as the crosslinker forming a rigid network to hold the QPMV copolymers. As shown in Table 1, the water uptake of the crosslinked QPMV was successfully reduced to approximately 60 wt% in fully water-saturated condition. AFM characterization was performed on both uncrosslinked and crosslinked QPMV membranes to learn the nano-scale morphologies of the membranes. Fig. 10a and b are the 3D topography and 3D phase image of the uncrosslinked QPMV membrane, respectively. Fig. 10c and d are the 3D topography and 3D phase image of the crosslinked QPMV membrane, respectively. It was found that the crosslinked membrane, as shown in Fig. 10c, had a rougher surface compared with the uncrosslinked one (Fig. 10a). The 3D phase image of the uncrosslinked QPMV (Fig. 10b) shows a distinct phase separation induced by the amphiphilicity of MMA and quaternized VBC. The peak regions represented the hydrophobic domains and the valley regions represented the

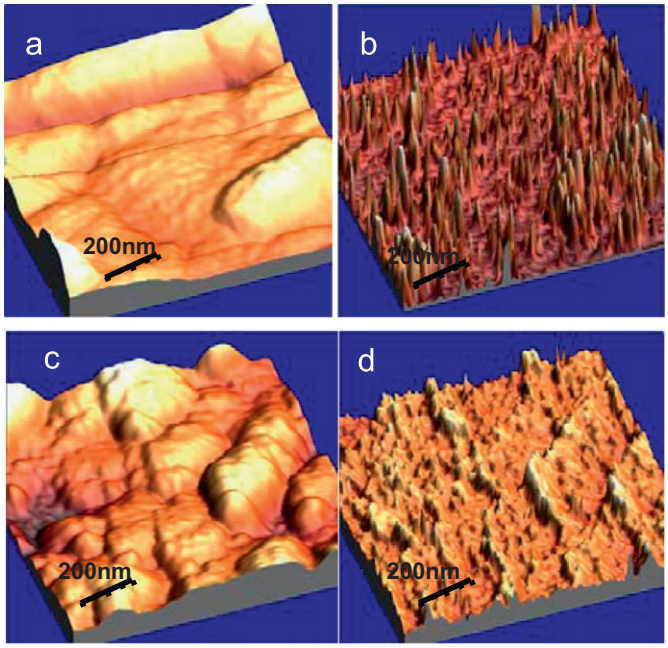

Fig. 10. AFM images for both uncrosslinked and crosslinked QPMVs. (a) 3D topography of the uncrosslinked QPMV membrane; (b) 3D phase image of uncrosslinked QPMV; (c) 3D topography of the crosslinked QPMV membrane; (d) 3D phase image of crosslinked QPMV.

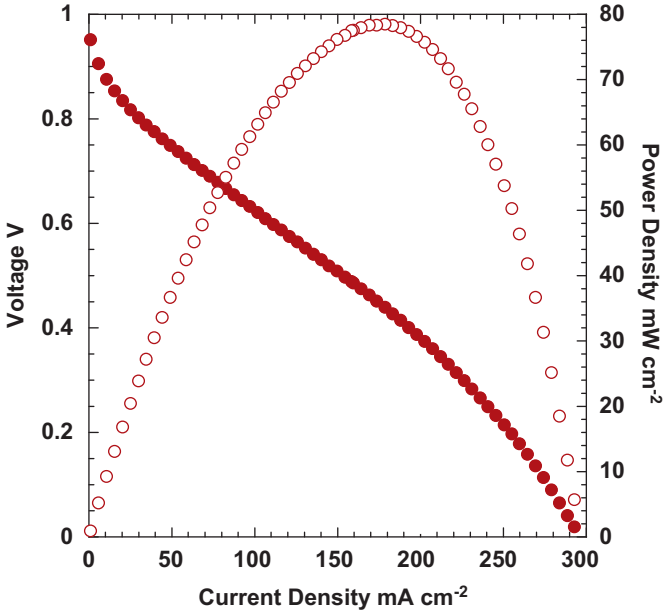

Fig. 11. Polarization curve of 10% crosslinked AAEM at 70 °C.

hydrophilic ionic conducting domains. In Fig. 10d, the phase separation was not as distinct as that shown in the uncrosslinked membrane. However, the 3D phase image showed that the phase separation still occurred, as the conducting domains were still homogeneously dispersed. The difference between Fig. 10b and d was that the contrast between the hydrophobic portion (peaks) and the hydrophilic ionic channels (valleys) became less distinct. This observation can certainly be attributed to crosslinking the polymer: the less distinct phase separation was due to more rigid polymer network in the crosslinked membrane, which was hence helpful to resist water-uptake.

To demonstrate the feasibility of the AAEM for practical AFC applications, the 10% crosslinked AAEM was tested in a fuel cell assembly for its polarization performance and power density. Prior to fuel cell tests, the dry metal-ion free AAEM was sandwiched by two 5 cm^2 catalyst loaded (Pt loading of 0.4 ± 0.05 mg cm^{-2}) carbon papers with hot-press. Hydrogen and pure oxygen was used as the fuel and oxidant in the test, respectively. The obtained polarization curve is plotted in Fig. 11, which demonstrated the maximum current density of 300 mA cm^{-2} at 70 °C with a peak power density of 80 mW cm^{-2}.

4. Conclusion

Based on the detailed study on the effects of copolymer composition drift, molecular eight, and copolymer crosslinking, the properties of QPMV-based AAEM were optimized. Quantitative correlation between the initial monomer ratio and the resulted copolymer composition has been established to predict the ratio of hydrophobic/hydrophilic portions in the obtained membranes. The effect of initiator and surfactant concentrations on molecular weight was also investigated. Decreasing initiator KPS and increasing surfactant SDS could be effectively increase the molecular weight, leading to improved mechanical properties including Young's modulus and tensile strength. Moreover, crosslinking method was employed to alleviate the water uptake problem. AFM characterization indicated that the crosslinked membranes has less distinct phase separation feature, which was believed to be the reason of well controlled water-uptake to resist the membrane deformation.

Acknowledgments

This research was supported by Army Research Lab (W911NF0920007) and Army Research Office (W911NF0910028). The authors were grateful to Prof. P. Kofinas and Prof. S.R. Raghavan at the University of Maryland for the technical support of polymer characterization.

References

[1] R. O'Hayre, S. Cha, W. Colella, F. Prinz, Fuel Cell Fundamentals, first edition, John Wiley & Sons, Inc., 2006, pp. 240.
[2] G. Maclean, T. Niet, S. Prince-Richard, N. Djilali, Int. J. Hydrogen Energy 27 (2002) 507.
[3] J. Varcoe, R. Slade, Fuel Cells 5 (2005) 187.
[4] S. Lu, J. Pan, A. Huang, L. Zhuang, J. Lu, PNAS 105 (2008) 20611.
[5] J. Zhou, M. Unlu, J.A. Vega, P.A. Kohl, J. Power Sources 190 (2009) 285.
[6] Y. Xiong, Q. Liu, Q. Zeng, J. Power Sources 193 (2009) 541.
[7] G. Wang, Y. Weng, J. Zhao, R. Chen, D. Xie, J. Appl. Polym. Sci. 112 (2009) 721.
[8] L. Li, Y. Wang, J. Membr. Sci. 262 (2005) 1.
[9] J. Fang, P. Shen, J. Membr. Sci. 285 (2006) 317.
[10] L. Wu, T. Xu, D. Wu, X. Zheng, J. Membr. Sci. 310 (2008) 577.
[11] M.R. Hibbs, C.H. Fujimoto, C.J. Cornelius, Macromolecules 42 (2009) 8316.
[12] B. Lin, L. Qiu, J. Lu, F. Yan, Chem. Mater. 22 (2010) 6718.
[13] L. Wu, T. Xu, J. Membr. Sci. 322 (2008) 286.
[14] Y. Wan, K. Creber, B. Peppley, V. Bui, J. Membr. Sci. 284 (2006) 331.
[15] Y. Wan, B. Peppley, K. Creber, V. Bui, E. Halliop, J. Power Sources 162 (2006) 105.
[16] J. Wang, R. He, Q. Che, J. Colloid Interface Sci. 361 (2011) 219.
[17] J. Zhou, M. Unlu, I. Anestis-Richard, P. Kohl, J. Membr. Sci. 350 (2010) 286.
[18] C. Sollogoub, A. Guinault, C. Bonnebat, M. Bennjima, L. Akrour, J. Fauvarque, L. Ogier, J. Membr. Sci. 335 (2009) 37.
[19] H. Xu, J. Fang, M. Guo, X. Lu, X. Wei, S. Tu, J. Membr. Sci. 354 (2010) 206.
[20] H. Kostalik IV, T. Clark, N. Robertson, P. Mutolo, J. Longo, H. Abruna, G. Coates, Macromolecules 43 (2010) 7147.
[21] Y. Luo, J. Guo, C. Wang, D. Chu, J. Power Sources 195 (2010) 3765.
[22] Y. Luo, J. Guo, C. Wang, D. Chu, ChemSusChem 11 (2011) 1557.
[23] Y. Luo, J. Guo, C. Wang, D. Chu, Macromol. Chem. Phys. 212 (2011) 2094.
[24] Y. Luo, J. Guo, C. Wang, D. Chu, Electrochem. Commun. 16 (2012) 65.
[25] Z. Pan, Polymer Chemistry, third edition, Chemical Industry Press, 2003 pp. 41.
[26] P. Painter, M. Coleman, Fundamentals of Polymer Science, second edition, CRC Press LLC, 1997, pp. 107.